

DEVELOPMENT OF RASTER SCANNING SYSTEM AT NIRS-HIMAC

T. Furukawa[#], T. Inaniwa, S. Sato, N. Saotome, S. Fukuda, T. Shirai, Y. Takei, Y. Iwata, A. Nagano, S. Mori, S. Minohara, T. Murakami, E. Takada and K. Noda
 National Institute of Radiological Sciences, Chiba, JAPAN
 Y. Iseki, K. Hanawa, N. Kakutani, C. Yamazaki, Y. Kanai
 Toshiba, Tokyo, JAPAN
 H. Izumiya and Y. Sano
 Accelerator Engineering Corp., Chiba, JAPAN

Abstract

A new treatment facility project, as an extension of the existing HIMAC facility, has been initiated for the further development of carbon-ion therapy in NIRS. This new treatment facility will be equipped with a 3D irradiation system with pencil beam scanning. The challenge of this project is to realize treatment of a moving target by scanning irradiation. To accomplish practical moving target irradiation and to fix the final design, a prototype of the scanning irradiation system was constructed and installed into existing HIMAC experiment course. The system and the status of the beam test are described.

INTRODUCTION

Heavy-ion beams have attracted growing interest for cancer treatment due to their high dose localization and high biological effect at the Bragg peak. To make optimal use of these characteristics and achieve accurate treatment, 3D pencil beam scanning [1-3] is one of sophisticated techniques, and it has already been utilized for treatment at the PSI [2] and GSI [3]. At HIMAC, a project [4] to construct a new treatment facility was initiated for implementation of this irradiation technique. The challenge of this project is to realize treatment of a moving target by scanning irradiation, because pencil beam scanning is more sensitive to organ motions compared with the conventional broad-beam irradiation. Design study of the scanning system had been started in 2006. One of the most important features of the system is fast scanning to realize moving target irradiation with a relatively large number of rescanning within an acceptable irradiation time. As a result of the conceptual design study [5], we decided to employ the hybrid raster scanning method similar to GSI [3] considering the beam characteristics of the HIMAC synchrotron [6]. Further, we found that the specification of the raster scanning system strongly depends on the specifications of following components: 1) fast scanning magnet and its power supply, 2) high-speed control system and 3) beam monitoring. Thus, we focused on the detailed design and the fabrication of these components. The prototype of the scanning system was constructed and installed in physics experiment course (PH1) of HIMAC in Dec. 2008. Fig. 1 shows the photograph of the prototype.

On the other hand, following developments are carried

out toward fast scanning: 1) Treatment planning for fast scanning and 2) modification of synchrotron control. The technical details of them are referred to [7, 8] and [9]. Our goal is to achieve the irradiation time of moving target to be less than few minutes for 10 times rescanning with gating.

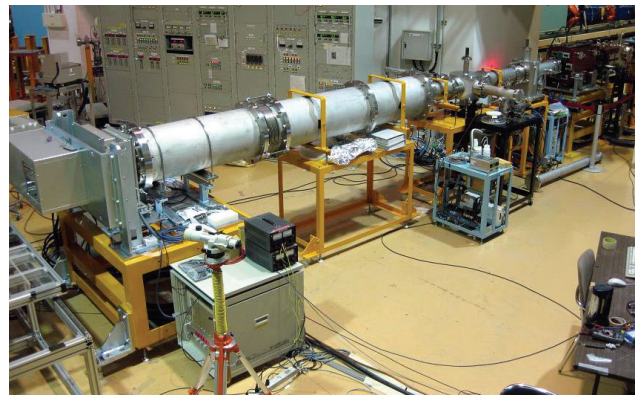


Figure 1: Photograph of the prototype of the raster scanning system.

PROTOTYPE OF SCANNING SYSTEM

Layout of Devices

The raster scanning irradiation system is around 9 m long between the last quadrupole magnet and the iso-center. The distances from both scanning magnets to the iso-center are set to 8.4 and 7.6 m, respectively. After the vacuum window located 1.3 m upstream of the iso-center, flux monitors, a position monitor, a ridge filter, and a range shifter are placed. Details of these components are described below.

Fast Scanning Magnet and its Power Supply

Specifications of the scanning magnets and their power supply are summarized in Table 1. The gap of the magnets and the good field region are defined based on the beam envelope calculation. The maximum magnetic field of both magnets is designed to be less than 0.3 T to decrease the eddy current and the iron losses. In addition, the silicon-steel lamination thickness of 0.35 mm was employed. Vacuum ducts in the scanning magnets are made of 4 mm-thick FRP to suppress the eddy current due to the ramping magnetic field. Consequently, the fast scanning velocity more than 100 mm/ms is realized.

[#] t_furu@nirs.go.jp

In order to check the eddy current effect especially for the magnet edge, measurement of the temperature rise was carried out. Fig. 2 shows the pictures of the horizontal and vertical scanning magnets before the installation and the typical result of the temperature rise measurement for the horizontal scanning magnet. The temperature rise was not severe, even when operating at the maximum field and repetition rate.

Table 1: Specifications of Scanning Magnets and their Power Supply

	unit	SMx	SMy
Deflection angle	mrad	±18	±21
Magnet gap width	mm	40	82
Effective length	mm	393.6	681.2
Pole length	mm	360	618
Pole width	mm	90	140
Max. field strength	T	0.286	0.190
Num. of coil-turns	turns/pole	12	15
Coil resistance	mΩ	5.6	10.3
Coil inductance	mH	0.94	2.02
Weight	kg	290	730
Max. current	A	±410	±440
Max. voltage	V	420	460
Scan speed	mm/ms	> 100	> 50

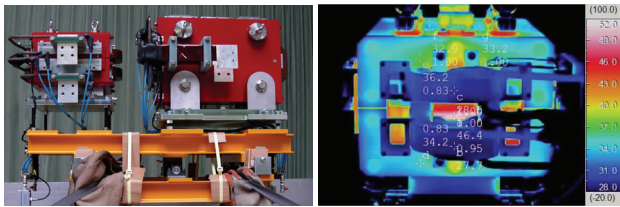


Figure 2: Pictures of the scanning magnets and the result of the temperature-rise measurement.

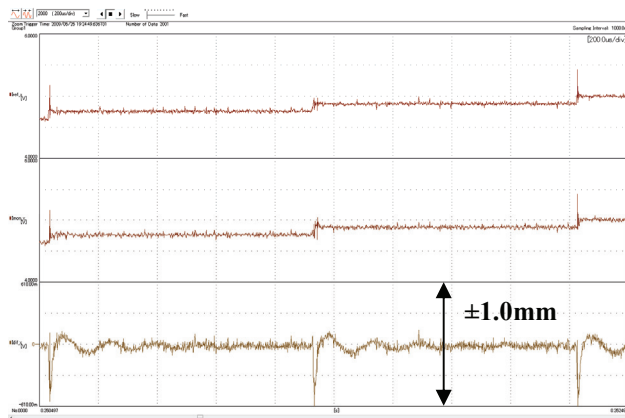


Figure 3: Oscilloscope display in the power supply test. From the upper trace, the reference current, the measured current and the measured deviation. Time scale is 200 μs/division.

In the power supply, IGBT units and FET units are employed, and separated functionally. The IGBT units are

used to change the current fast, and the FET units are used to keep the current constant with the PID feedback control. The fast control of the IGBT units is the most crucial issue of this power supply. The switching timing precision of around 300 ns is necessary to suppress over/under shoot. As shown in Fig. 3, the overshoot is successfully suppressed within 0.5 A corresponding to the beam-position shift of 0.2 mm. Consequently, FET units can control such over/under shoot within 100 μs.

Beam Monitors

The beam monitoring is one of the most important components in the scanning delivery. In order to measure and control the dose of each spot, two flux monitors (principal and subordinate) and a beam position monitor will be placed. However, a sub flux monitor and the position monitor are not yet installed in this stage, and will be installed soon. The flux monitors are parallel-plate ionization chambers with an effective area of 240 mm². The beam position and profile are measured with a multi wire proportional counter (MWPC), which will be set just after the main and sub monitors. While the MWPC needs to have controlled gas flow, the flux monitor operates in air. The flux monitor consists of a signal foil, two HV foils and two grounded shielding foils. Each foil is made of 50 μm-thick polyimide coated by Cu, Ni and Au. The gap between signal and HV foils is 4 mm on both sides of the signal foil. The output current from the flux monitor is digitized by the current-frequency converter having maximum frequency of 2 MHz.

Mini Ridge Filter and Range Shifter

The Bragg peak of the pristine beam is slightly broadened to produce a “mini peak” by using a mini ridge filter (RGF). The shape of bar ridge is designed to make Gaussian shaped mini peak of 3 mm width at 1-sigma. The RGF consists of 160 bar ridges made of aluminium, and has an effective area of 240 mm². The distance between the RGF and the iso-center is set to be 1 m. Considering the RGF structure blurring [10] and the alignment accuracy of bar ridges, each bar ridge has the aluminium base plate of 1 mm thickness.

The range shifter (RSF) is used to precisely change the range slice-by-slice in the target. In order to reduce the beam size expansion by multiple scattering, the RSF is located close to the iso-center. The entrance and exit of RSF are 0.9 and 0.6 m upstream of the iso-center, respectively. This binary type RSF consists of ten acrylic plates. Each plate has the thickness of 0.2 ~ 102.4 mm with an effective area of 240 mm². By using the compressed-air cylinder, it takes around 300 ms to move/remove each plate.

Control System for Scanning Delivery

The scanning beam delivery is realized by the specific controllers that consist of the high-speed control part (order of few hundred ns) and the low-speed control part (order of few ms). The high-speed part consists of the FPGA and memory modules, on the VME board, and

controls the irradiation dose and the position of each spot. Concerning reliability of the system, the CPU on the VME is only used to download the scanning steering data to the memory modules, and not used to control the scanning delivery. Since the memory modules need to memorize the steering data including the rescannings, each memory module has the memory area for 22M spots. The steering data are delivered through the gigabit network. On the other hand, the low-speed part consists of the programmable logic controllers (PLC) and their I/O modules. This part controls and monitors the components having slow response, such as the RSF, the HV, and the monitor gas.

BEAM TEST

Commissioning of the prototype started in December 2008. Cooperating with highly stabilized beam provided by HIMAC, the commissioning is successfully in progress. Since the measured beam property is employed in the treatment planning calculation [7, 8], firstly, pencil beam measurement was carried out by using a cylinder type water column with ionization chambers. The cylinder type water column is a sealed tank of the water for the depth dose curve measurement. The detectors are the large area parallel plate ionization chamber and the 94 channel cross-shaped monitor, not only for the integral depth dose curve measurement, but also for the lateral dose distribution. Both detectors are set in the same case made of aluminum having the grounded shielding window. Fig. 4 shows the typical result of pencil beam measurement and its modelling.

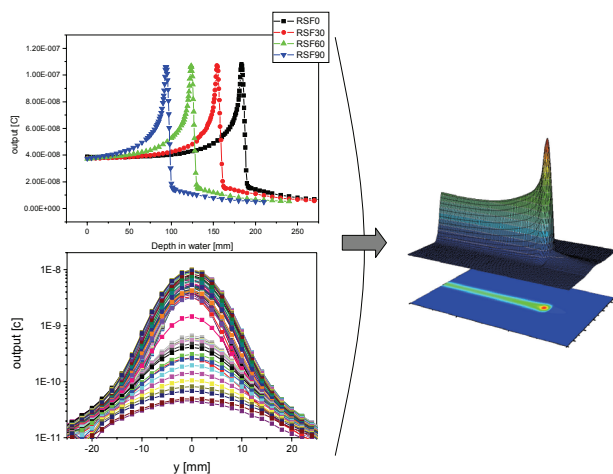


Figure 4: Typical result of pencil beam measurement and its modelling for dose calculation in the treatment planning.

A fluorescent screen with CCD camera [11] is a very useful tool for 2D measurement in the scanning delivery verification. By applying calibration using the film measurement, it was possible to remove artefacts from 2-D images caused by variations in the pixel-to-pixel sensitivity of the detector or screen and by distortions in the optical path between the screen and the detector. We

employ this device for 1) calibration of the scanning magnet deflection, 2) observation of beam symmetric property and 3) check of lateral uniformity of delivered field. Fig. 5 shows typical results of 1) and 3).

For the verification of 3D delivery, the box shaped target of $60 \times 60 \times 60$ mm³ was planned to generate uniform physical dose field of 1 Gy. As shown in Fig. 6, the dose distributions measured by ionization chamber were in good agreement with the planned one at various penetration depths.

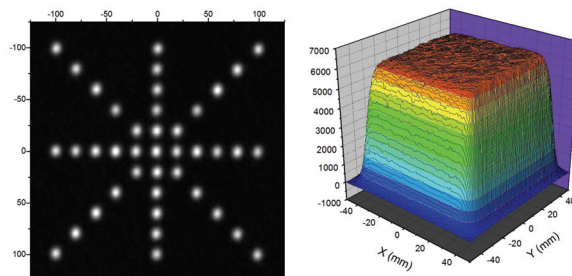


Figure 5: Measured images by the fluorescent screen system.

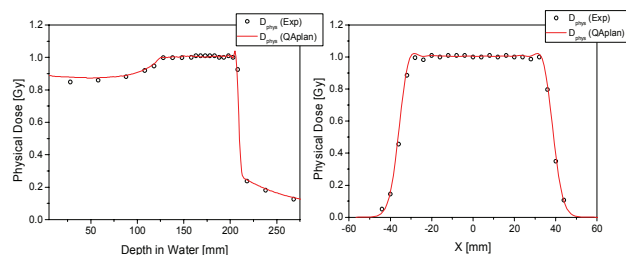


Figure 6: Comparison between measured (open circle) and planned (line) dose distribution.

SUMMARY

The beam tests of the scanning prototype for the HIMAC new treatment facility are well underway. Until end of 2009, the beam test will be continued including the moving phantom irradiation. After the small modification, this prototype will be installed in the new facility.

ACKNOWLEDGEMENTS

We would like to express our thanks to members of Accelerator Engineering Corporation for their skilful operation of the HIMAC accelerator complex. We would also like to express our thanks to other members of Department of Accelerator and Medical Physics at NIRS for useful discussion. This work was carried out as a part of Research Project with Heavy Ions at NIRS-HIMAC.

REFERENCES

- [1] T. Kanai et al, Nucl. Instr. Meth. 214 (1983) 491.
- [2] E. Pedroni et al, Med. Phys. 22 (1995) 37.
- [3] Th. Haberer et al, Nucl. Instr. Meth. A 330 (1993) 296.
- [4] K. Noda et al, Proc. of EPAC 2008, 1818.

- [5] T. Furukawa et al, Med. Phys. 34 (2007) 1085.
- [6] T. Furukawa et al, Nucl. Instr. Meth. A560 (2006) 191.
- [7] T. Inaniwa et al, Med. Phys. 34 (2007) 3302.
- [8] T. Inaniwa et al, in these proceedings.
- [9] Y. Iwata et al, Proc. of EPAC 2008, 1800.
- [10] U. Weber, G. Kraft, Phys. Med. Biol. 44 (1999) 2765.
- [11] N. Saotome et al, Proc. of EPAC 2008, 1830.